Proc. Natl. Acad. Sci. USA
Vol. 85, pp. 5062–5066, July 1988
Biophysics

Iron–carbonyl bond geometries of carboxymyoglobin and carboxyhemoglobin in solution determined by picosecond time-resolved infrared spectroscopy

(heme proteins/polarized infrared spectroscopy/heme-ligand geometry)

JOHN N. MOORE, PATRICIA A. HANSEN, AND ROBIN M. HOCHSTRASSER

Department of Chemistry, University of Pennsylvania, Philadelphia, PA 19104

Contributed by Robin M. Hochstrasser, March 21, 1988

ABSTRACT **The iron–carbonyl geometries in carboxymyoglobin (MbCO) and carboxyhemoglobin (HbCO) in ambient temperature solution have been investigated using picosecond time-resolved infrared spectroscopy. Polarized infrared and visible beams were used to monitor the change in infrared absorbance of the bound CO stretch bands on photodissociation of the ligand. The ratio of the change in absorbance for perpendicular and parallel relative polarizations of the photolysis and infrared probe beams is directly related to the angle between the ligand bond axis and the normal to the heme plane. Ratios, and hence the angles, have been obtained for the configurations giving rise to the principal CO stretch infrared absorption bands of HbCO and MbCO: 18° for the 1951 cm^{-1} band of HbCO; 20° and 35°, respectively, for the 1944 cm^{-1} and 1933 cm^{-1} bands of MbCO. Structures consistent with x-ray diffraction and the picosecond experiments reported here are proposed for MbCO and HbCO in which the Fe—C bond tilts to the heme normal and the Fe—C—O angle differs significantly from 180°.**

The infrared (IR) spectra of carboxyheme proteins in the region of the carbonyl stretching frequency indicate plausible heme–ligand structures (1). Knowledge of these structures for heme proteins in solution is needed to fully understand how the protein influences the ligand dynamics. It is therefore important to generate new experiments that help establish the relationships between observed IR spectra and heme–ligand structure.

We have recently suggested a new method of determining IR spectra with ps time resolution (2). In this measurement the sample is first pumped by a ps pulse of visible or UV light and the IR spectrum of the sample consisting of both photoproducts and unphotolyzed material can be recorded at variable ps delay times. The experiment can be done with polarized IR and visible beams, so that the magnitude and decay of the orientational correlation function for photoproducts and unphotolyzed material can be evaluated. For heme proteins—where the overall molecular rotation is slow—the magnitude of the polarization anisotropy is directly related to the angle between the transition dipoles for the IR and visible absorptions. In this paper we present results from a significantly improved version of the original experimental design, applied to the photodissociation of carboxymyoglobin (MbCO) and carboxyhemoglobin (HbCO). The measurements are used to define the heme–CO geometry for these heme proteins in solution. The preliminary results (2) for MbCO involved an uncertainty in the polarization anisotropy of >50%. In this study the error is reduced to ≈10% and allows a sharp definition of the ligand geometry of this heme protein in solution.

The publication costs of this article were defrayed in part by page charge payment. This article must therefore be hereby marked "*advertisement*" in accordance with 18 U.S.C. §1734 solely to indicate this fact.

MATERIALS AND METHODS

Spectroscopic Method. The transient IR spectra were recorded using the same principles as previously described (2). The sample is photolyzed by means of a pulse from a dye laser that is synchronously pumped by the frequency-doubled output of a mode-locked and Q-switched Nd:YAG laser. A single pulse (558 nm, 25 ps, 5 μJ) is selected from the dye laser at a repetition rate of ≈250 Hz. The IR source is a CW diode laser (Spectra Physics, Laser Analytics Division, Bedford, MA) that can be tuned from 1900–2000 cm^{-1}, the carbonyl stretch region for heme proteins. The IR beam is passed through the sample colinear with the photolyzing beam, and the changes induced in the IR as a result of optical pumping are interrogated by sum-frequency mixing the transmitted IR with a pulse (561 nm, 20 ps, 1 μJ) from a second ps dye laser in a nonlinear crystal of $LiIO_3$. This mixing upconverts the IR signal to the visible range, where it can be detected with a photomultiplier tube. The single pulse from the upconverting dye laser is selected in synchrony with that from the photolyzing dye laser. The two dye lasers can be variably delayed at a fixed diode laser frequency such that the intensity–time profile of the IR beam, and thus the kinetics of the chosen transition, can be directly measured. Alternatively, with the optical delay line at a particular setting, τ, the diode laser can be frequency scanned to yield the IR spectrum corresponding to time τ after photolysis.

A custom-built bandpass filter was used to separate the upconverted IR signal from that of the second dye laser, resulting in an improvement of about one order of magnitude in signal compared with that obtained with a monochromator. In the polarization experiment the change in IR absorbance at a particular time delay is first measured with the photolyzing beam and detected IR signal having the same polarization ($\Delta A_{\parallel}$) and then with their polarizations perpendicular ($\Delta A_{\perp}$).

In the present experiment the polarization changes were made by rotating a $\lambda/2$ plate placed in the photolyzing beam; this technique significantly improved reproducibility.

The polarization experiment was carried out as follows. The upconversion signal intensity was measured both with the photolyzing beam blocked and with the photolyzing beam incident on the sample. The $\lambda/2$ plate in the photolyzing beam was then rotated such that the polarization of that beam was rotated by 90°, and the signal measurements were repeated. In this way, the change in IR absorbance could be measured for both parallel and perpendicular IR/photolysis laser polarizations. Measurements were taken using a time delay of 40 ps between the pump and probe lasers. A correction factor of ≈5% was required to compensate for the difference in reflectance for the two polarizations of the dichroic beam

Abbreviations: MbCO, carboxymyoglobin; HbCO, carboxyhemoglobin.

splitter used to direct the photolyzing beam to the sample, and this is incorporated into the reported values.

Improvements were also made in the experiment by introducing a controlled sample flow and reducing the repetition rate of the photolyzing beam to ≈250 Hz to ensure that there was no observation of any steady-state photolysis. This technique has eliminated the occurrence of interference between signals from successive pulses, which contributed to large uncertainties in the earlier measurement.

Preparation of Materials. The samples were prepared by dissolving sperm whale myoglobin, Mb, and human hemoglobin, Hb (Sigma), in potassium phosphate buffer at pH 7. Both samples were stirred for several hours under a CO atmosphere, reduced with sodium dithionite, and stirred under CO for several more hours to form the carboxy derivatives. Final concentrations were ≈15 mM.

RESULTS

Results are given in Table 1. For HbCO the principal carbonyl absorption is a single line at 1951 cm^{-1}, whereas for MbCO we see two lines at 1944 cm^{-1} and 1933 cm^{-1}. Conventional IR spectra show two lines and three lines, respectively (Table 2), with the strongest ones corresponding to those that we observe. Values of $R = \Delta A_\perp/\Delta A_\parallel$ given in Table 1 are the mean values for data sets consisting of ≈20 measurements, with uncertainties of about 9–16%; this error stems principally from photon noise from low signal intensities and fluctuations in the diode laser intensity. Variation in R between separate data sets is typically ±5%.

Values for the angle α are also included in Table 1. The angle α value corresponds to the best estimate for an angle between the carbonyl bond axis and the normal to the heme plane from interpreting the anisotropic absorption as follows: Absorption changes for infinitesimally short light pulses, $\Delta A^\circ_\parallel$ and $\Delta A^\circ_\perp$, are assumed to result from depleting the carboxyheme population by dissociation of CO after absorption of a polarized visible photon into the doubly degenerate (x,y polarized) Q band of the heme. The colinear probe IR beam, polarized parallel or perpendicular to the photolyzing beam, is assumed to interact through a transition dipole along the C—O bond axis that makes an angle α with the normal to the heme plane. The anisotropy $r(t)$ defined (6) as $(\Delta A^\circ_\parallel - \Delta A^\circ_\perp)/(\Delta A^\circ_\parallel + 2\Delta A^\circ_\perp)$ is given by:

$$r(t) = \frac{2}{5}\langle P_2[\hat{\mu}_{ABS}(0)\cdot\hat{\alpha}(t)]\rangle, \quad [1]$$

where $P_2(x)$ is the second Legendre polynomial $1/2\,(3x^2 - 1)$. The unit vectors $\hat{\mu}_{ABS}(0)$ and $\hat{\alpha}(t)$ correspond to the transition dipole directions for the photolyzing transition at time zero and the probed transition (in the IR) at time t after photolysis, respectively. The angled brackets signify an angular and ensemble average. For the degenerate transition, $r(t)$ is the average of the anisotropies for x- and y-polarized absorption:

$$r(t) = \frac{1}{2}[r_x(t) + r_y(t)], \quad [2]$$

Table 1. Polarization ratio R and corresponding angle α determined for MbCO and HbCO solutions at 295 K

Heme protein	ν(CO)/cm^{-1}	Polarization ratio R	Angle α, degrees
MbCO	1944	1.74 ± 0.16	20
	1933	1.38 ± 0.23	35
HbCO	1951	1.78 ± 0.23	18

Table 2. Reported values for the bound CO stretch bands and bandwidths (FWHM) of MbCO and HbCO under sample conditions similar to those of this study

Heme protein	ν(CO)/cm^{-1}	$\Delta\nu_{1/2}$/cm^{-1}	Relative intensity, %	Reference
MbCO	1967	8	<1	1, 3, 4
	1944	9	72	
	1933	10	28	
HbCO	1968	8	1–2	5, 3
	1951	8	98–99	

where $r_x(t) = 2/5\langle P_2[\hat{x}(0)\cdot\hat{\alpha}(t)]\rangle$. From the fact that $\cos^2\theta_{x\alpha} + \cos^2\theta_{y\alpha} + \cos^2\theta_{z\alpha} = 1$, it follows that:

$$r(t) = -\frac{1}{2}r_z(t), \quad [3]$$

where $r_z(t) = 2/5\langle P_2[\hat{z}(0)\cdot\hat{\alpha}(t)]\rangle$ and z is the direction perpendicular to the heme plane. Clearly $r(t)$ depends only on $\hat{z}(0)\cdot\hat{\alpha}(t) = \cos\alpha(t)$, where $\alpha(t)$ is the angle between the C—O bond at time t and the normal to the heme plane at time zero of the ground-state molecules of MbCO or HbCO. The polarization ratio $\Delta A^\circ_\perp/\Delta A^\circ_\parallel$ can therefore be written as:

$$\frac{\Delta A^\circ_\perp(t)}{\Delta A^\circ_\parallel(t)} = \frac{4 - \langle\sin^2\alpha(t)\rangle}{2 + 2\langle\sin^2\alpha(t)\rangle}, \quad [4]$$

where $\langle\text{---}\rangle$ indicate an average over the distribution of angles α. For finite-length laser pulses the observed ratio $R = \Delta A_\perp/\Delta A_\parallel$ is obtained by appropriately convoluting these pulse shapes with $\Delta A^\circ_\perp(t)$ and $\Delta A^\circ_\parallel(t)$ before taking the ratio. However, in the present case the rotational relaxation time of the heme is very long [≈8 ns for Mb (7) and ≈26 ns for Hb (8)] compared with the laser pulse widths (20 ps), so that if that is the only significant rotation of the relevant dipoles, we can identify $\Delta A^\circ_\parallel$ and $\Delta A^\circ_\perp$ with the observed values $\Delta A_\parallel$ and $\Delta A_\perp$. The polarization ratio is then independent of time for $t << 8$ ns and given by:

$$R = \frac{4 - \langle\sin^2\alpha\rangle}{2 + 2\langle\sin^2\alpha\rangle}, \quad [5]$$

where α is the angle between the C—O axis and the normal to the heme plane.

The correlation function in Eq. 1 gives the correct experimental anisotropy only when the photolyzing pulse introduces infinitesimal changes from the equilibrium orientational distribution. Strictly, the change in the ground-state population due to the photolyzing pulse is proportional to $\exp(-\sigma\varepsilon)$, where σ is the absorption coefficient and ε is the absorbed energy from the pulse (photons per cm^2). The small conversion limit holds if $\exp(-\sigma\varepsilon)$ is accurately given by $(1 - \sigma\varepsilon)$. In our experimental conditions, an error of ≤8% is introduced when only the first term in the expansion is used. However, it is straightforward to carry out the angular averages and also include the term in $(\sigma\varepsilon)^2$, such that the observed R values can be adjusted to those that would be observed in the limit of infinitesimal photolysis (9). This small correction is incorporated into the R values given in Table 1. Typically, the fraction of molecules photolyzed was ≈30%.

Values of α for HbCO and the 1944 cm^{-1} line of MbCO are the same within experimental error. The value of α for the MbCO 1933 cm^{-1} transition is significantly larger by about 15°.

The results in Table 1 are obtained by assuming a sharply peaked distribution of angles α. The bandwidths of CO stretch bands indicate the range of interactions between the ligand and its environment. For free hemes in solution these may be considerable, giving rise to IR bandwidths of up to 30 cm^{-1} (10). Such bandwidths may also be observed in heme

proteins, but in hemoglobins and myoglobins are typically $\approx 10\ cm^{-1}$ (11), as seen for the bands under study here (Table 2). This shows that there is a relatively uniform environment for the ligand in the conformation giving rise to each IR band and, hence, a relatively narrow distribution in the CO location. Furthermore, x-ray diffraction work shows well-defined oxygen positions (12, 13). The IR spectra for MbCO show the two strong CO peaks separated by 11 cm^{-1}. Our results indicate that α changes by 15° between the two configurations represented by these peaks. If the vibrational frequency were to change continuously with orientation, the observed spectral linewidth of each peak would place a limit on the SD in the distribution of angles for the CO group of 3.5°.

DISCUSSION

Several approaches have previously been used to study ligand orientation in heme proteins. X-ray and neutron diffraction and extended x-ray absorption fine structure (EXAFS) have been used to study crystals and low-temperature glasses, but no clear interpretation has evolved from such studies: The results can be fitted for a linear tilted, bent, or intermediate FeCO unit, as illustrated in Table 3 for MbCO and HbCO (12–17). The x-ray absorption near-edge structure (XANES) technique, being a sensitive probe of FeCO angle, although not to tilting of a linear unit, has obtained data both for crystals and solutions, as also given in Table 3 (18). Raman and IR methods have also been used extensively. In the case of the Raman method (19), the variation in the three FeCO vibrational frequencies with FeCO angle and isotopic substitution has been used to deduce a 5° bent unit for both MbCO and HbCO (20, 21). IR studies of the bound CO stretches of heme proteins have been numerous, particularly because this is a strong absorption in a clear region of the IR spectrum with respect to both solvent and other protein bands (11, 22). The summary of the bands observed for MbCO and HbCO given in Table 2 is for typical sample conditions used for IR spectroscopy, as employed in this work—i.e., pH 7, 295 K, and ≈15 mM. Bands seen in the present studies agree with values reported in the literature, although we note that the number, frequencies, bandwidths, relative intensities, and extinction coefficients of these bands in heme proteins vary, in general, with sample conditions such as pH, temperature, degree of hydration, crystal versus solution, and nature of crystal under study. The different IR bands observed have been assumed to correspond to different conformers. Angle changes, cis and trans effects, and electronic effects on the CO group caused by the environment of the metal ion or the CO itself can all affect the CO stretches, and there are, in general, no rules for the determination of metal–CO structures from CO stretch bands (23, 24). Estimates of FeCO structures have, nevertheless, been made from the study of the CO stretch spectral region under various sample conditions (1, 3, 5, 25, 26). It has generally been postulated that the high frequency bands (1967, 1968 cm^{-1}) correspond to conformers, present in very low concentration under normal solution conditions, in which the ligand is in a more open pocket and is consequently relatively upright and tightly bound (3, 5). This proposal has been supported by work using Raman spectroscopy (27). The remaining lower frequency bands have been assumed to correspond to the structures in which the CO is distorted from a linear, perpendicular configuration, and a commonly discussed effect of the heme pocket on the CO ligand has been that of interaction between the carbonyl group and the nitrogen atom of the distal histidine (E7), which can act as an electron donor and which is in close proximity to the ligand. It has been proposed that, in general, lower CO stretch frequencies correlate with an increase in nucleophilic donation from the histidine (1, 25), and this proposal has been used to account for the different kinetics of the two bands seen for recombination of photolyzed MbCO at low temperatures (28) where the 1944 cm^{-1} band was found to recover much more readily than the lower-frequency 1926 cm^{-1} band. The two bands have been proposed to correspond to relatively "open" and "closed" conformations of the pocket—the 1926 cm^{-1} band corresponding to the closed conformation, with the lower IR frequency being due to interaction with the distal histidine. The two conformations have also been suggested to correspond to the geometries with different dihedral angles seen by x-ray diffraction (12, 29).

The crystal structures of model porphyrin–CO compounds have shown an almost linear perpendicular FeCO unit ($\alpha <$ 3°) (30, 31) and, as indicated above, the distortion from this configuration is considered to be due to steric constraints caused by the heme pocket and not a change in electronic structure of the group resulting in a different preferred configuration. This idea is given strong support by our recent observations (2, 9) on protoheme–CO structures in solution. We have found that the CO is significantly inclined to the heme normal and that the amount of this inclination depends on the different solvent structures obtained as the viscosity is varied.

The energetics for distortion of the FeCO unit by means of either a tilt in which the FeCO axis remains linear, or a bend, in which the Fe—C axis remains perpendicular to the heme plane, have been estimated (32), and it was concluded that the protein matrix was not sufficiently rigid to bend the FeCO unit by >20° and that the tilt of a linear unit was the more likely distortion because this required less strain on the protein. Other calculations on model heme–CO complexes have suggested that a combined tilted and bent structure is most likely in the case of the heme proteins (33).

Table 3. Reported values for the FeCO configuration in MbCO and HbCO using neutron diffraction, x-ray diffraction, extended x-ray absorption fine structure, and x-ray absorption near-edge structure

Heme protein	Technique	FeCO configuration	Reference
MbCO (crystal)	ND	Bent 45°	14
MbCO (crystal)	ND	Linear tilted 24°	15
MbCO (crystal)	XD	Bent 40° and 60°	12
MbCO (glass)	EXAFS	Bent 53° (or 35°)	16, 17
MbCO (crystal and solution)	XANES	Bent 30°	18
HbCO (crystal)	XD	Linear tilted 14° (α)	13
HbCO (crystal)	XD	Linear tilted 13° (β)	13
HbCO (solution)	XANES	Bent 15°	18

The angles given are for the angles made between the CO and the heme normal. ND, neutron diffraction; XD, x-ray diffraction; EXAFS, extended x-ray absorption fine structure; XANES, x-ray absorption near-edge structure.

Polarized absorption spectra have been studied for a number of heme proteins and ligands (34). The relevance of these studies to the work described here is their determination of the transition moments of the visible absorption Q bands in the 500- to 600-nm region. The absorption in this region for MbCO and HbCO is x,y-polarized in the plane of the heme, but the Q_0 band (≈570 nm) has unequal x and y components. Outside this band the x and y components are equal (34–36), and the heme behaves as a circular absorber—i.e., there is equal probability of absorption for all directions of the electric vector of the radiation parallel to the heme plane. Because the results reported here are more easily interpreted for a circular absorber, the wavelength of the photolysis laser employed was 558 nm, outside the Q_0 band, and in the region where the assumption that the heme is a circular absorber is valid.

The assumption that the CO stretch is polarized along the CO bond axis is commonly made because the CO behaves to good approximation as a local oscillator (19, 23, 24). This assumption has been made in many other studies with polarized IR spectroscopy as a probe of CO orientation—examples being CO adsorbed on surfaces (37) and CO units in larger molecules adsorbed on surfaces (38), and this assumption is made here.

The two assumptions regarding heme and CO transition dipoles form the basis for the interpretation of the anisotropic change in IR absorbance to obtain the angles of the CO to the heme normal. Our experimental procedure distinguishes only between different values of α for the angle of the CO to the normal of the heme plane and not between different configurations (bent, linear tilted, or a combination of the two) with the same α value. Neither does the technique distinguish between configurations with different values of the dihedral angle in the molecule frame. From consideration of previous work, as given above, either the simple bent or linear tilted cases would probably not describe the actual case in the protein, which is most likely a combination of the two.

The significant result of these studies is that the angle of the CO ligand to the normal of the heme plane has been determined accurately for the configurations corresponding to the lower frequency IR bands of HbCO and MbCO in ambient temperature solution. It is reasonable to assume that the two configurations for MbCO measured here correspond to the two configurations obtained from x-ray diffraction studies (12), which have different dihedral angles. The x-ray results were modeled for a bent configuration, giving α values of 40° and 60°. However, the authors noted that at their resolution it was not possible to determine whether a linear tilted or a bent fit was the more suitable.

The FeCO configuration of MbCO and HbCO can be obtained by using the α values obtained here in conjunction with the FeO positions obtained from x-ray diffraction work on crystals. Although the IR spectra of crystals and solutions differ, these differences have been attributed to changes in the relative proportions of the same FeCO conformers and not to differences in crystal and solution structures. As stated above, the x-ray studies could define the oxygen position accurately, but could not define that of the carbon atom. Hence, by taking the α values from this study and the oxygen positions from x-ray work (12, 13) and setting the CO bond length at 1.12 Å as found in model compounds (30), we can obtain the FeCO configurations given in Fig. 1 and Table 4. All configurations have a combined bent and tilted structure. The geometries of the HbCO and MbCO systems are similar for the most prevalent configurations, and the observation of two significantly different structures for the two prominent IR bands of MbCO is a direct observation confirming the hypothesis that different IR bands correspond to different configurations of the FeCO unit. The postulate that a decrease in IR frequency corresponds to an increase in distortion from a linear perpendicular configuration is also confirmed in this case.

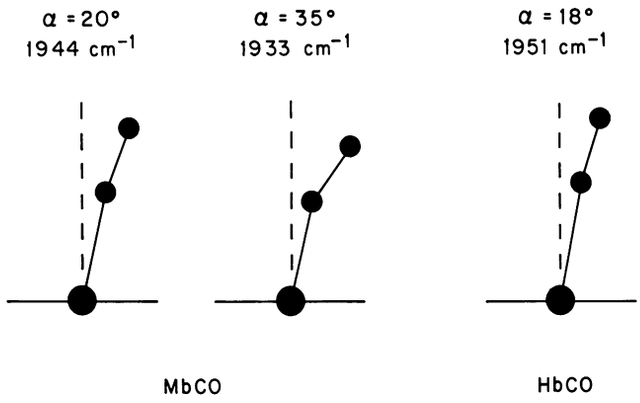

FIG. 1. FeCO configurations of MbCO and HbCO obtained with α values from this study in combination with FeO positions from x-ray diffraction work. —, Heme planes; ●, iron atoms; --, heme normals; •, CO molecules.

The distorted FeCO structures that we have now seen for these heme proteins undergo different geminate rebinding behavior from the protoheme distorted structures (2, 9). In the latter case most of the CO rebinds at high viscosities (39) on the time scale of 10^2 ps (2). For the heme proteins no significant sub-ns rebinding of CO occurs (40, 41). This suggests that the protein relaxation after deligation, which was recently analyzed using x-ray diffraction (12), introduces a steric barrier to rebinding in addition to the electronic barriers that may also exist from spin constraints (42). The protoheme would then illustrate the dynamics expected in the absence of a steric barrier. We note that O_2 has a reported sub-ns geminate recombination with Hb (42) and Mb (43), suggesting that the O_2 finds pathways to binding in the relaxed protein that are significantly less probable for CO. This difference could result from a significantly lower energy barrier for O_2 approaching Fe on trajectories of large angle between the O_2 axis and the heme plane, agreeing with Szabo's suggestions (44). Oxygen bonds to the heme at an angle to the normal, even in unstrained model compounds for which the CO is upright (45–47).

Technical assistance from Laser Analytics is gratefully acknowledged. This research was supported by grants from the National

Table 4. Estimated values for the distances and angles in the FeCO units of MbCO and HbCO

		MbCO		HbCO
IR data*	ν(CO)/cm^{-1}	1944	1933	1951
	α, degrees	20	35	18
XD data†	FeO/Å	2.88	2.77	3.10
	⊥O/Å	0.80	1.00	0.70
	Ø, degrees	60	−62	4, 19
	FeC/Å	1.77	1.70	1.98
	⊥C/Å	0.42	0.36	0.35
	FeCO, degrees	174	157	172
	⊥FeC, degrees	14	12	10

Values were obtained by using the α values of this study in combination with the positions of the carbonyl oxygen atom from x-ray diffraction work. The CO bond length is set at 1.12 Å, as found in a model compound (30). ⊥ indicates the normal to the heme plane through the Fe atom.

*Data from present work.

†Data from x-ray diffraction (XD) work; MbCO (12) and HbCO (13). Ø as defined in ref. 12.

Science Foundation (CHE-8603672) and the National Institutes of Health (GM12592).

1. Makinen, M. W., Houtchens, R. A. & Caughey, W. S. (1979) *Proc. Natl. Acad. Sci. USA* **76,** 6042–6046.
2. Moore, J. N., Hansen, P. A. & Hochstrasser, R. M. (1987) *Chem. Phys. Lett.* **138,** 110–114.
3. Brown, W. E., Sutcliffe, J. W. & Pulsinelli, P. D. (1983) *Biochemistry* **22,** 2914–2923.
4. Alben, J. O., Beece, D., Bowne, S. F., Doster, W., Eisenstein, L., Frauenfelder, H., Good, D., McDonald, J. D., Marden, M. C., Moh, P. P., Reinisch, L., Reynolds, A. H., Shyamsunder, E. & Yue, K. T. (1982) *Proc. Natl. Acad. Sci. USA* **79,** 3744–3748.
5. Choc, M. G. & Caughey, W. S. (1981) *J. Biol. Chem.* **256,** 1831–1838.
6. Szabo, A. (1984) *J. Chem. Phys.* **81,** 150–167.
7. Albani, J. & Alpert, B. (1986) *Chem. Phys. Lett.* **131,** 147–152.
8. McCalley, R. C., Shimshick, E. J. & McConnell, H. M. (1972) *Chem. Phys. Lett.* **13,** 115–119.
9. Hansen, P. A., Moore, J. N. & Hochstrasser, R. M. (1988) *Chem. Phys.*, in press.
10. Maxwell, J. C. & Caughey, W. S. (1976) *Biochemistry* **15,** 388–396.
11. Maxwell, J. C. & Caughey, W. S. (1978) *Methods Enzymol.* **54,** 302–323.
12. Kuriyan, J., Wilz, S., Karplus, M. & Petsko, G. A. (1986) *J. Mol. Biol.* **192,** 133–154.
13. Baldwin, J. (1980) *J. Mol. Biol.* **136,** 103–128.
14. Norvell, J. C., Nunes, A. C. & Schoenborn, B. P. (1975) *Science* **190,** 568–570.
15. Hanson, J. C. & Schoenborn, B. P. (1981) *J. Mol. Biol.* **153,** 117–146.
16. Chance, B., Fischetti, R. & Powers, L. (1983) *Biochemistry* **22,** 3820–3829.
17. Powers, L., Sessler, J. L., Wollery, G. L. & Chance, B. (1984) *Biochemistry* **23,** 5519–5523.
18. Biancóni, A., Congiu-Castellano, A., Durham, P. J., Hasnain, S. S. & Phillips, S. (1985) *Nature (London)* **318,** 685–687.
19. Yu, N.-T. (1986) *Methods Enzymol.* **130,** 350–409.
20. Tsubaki, M., Srivastava, R. B. & Yu, N.-T. (1982) *Biochemistry* **21,** 1132–1140.
21. Yu, N.-T., Kerr, E. A., Ward, B. & Chang, C. K. (1983) *Biochemistry* **22,** 4534–4540.
22. Parker, F. S. (1983) *Applications of Infrared, Raman and Resonance Raman Spectroscopy in Biochemistry* (Plenum, New York).
23. Braterman, P. S. (1975) *Metal Carbonyl Spectra* (Academic, London).
24. Braterman, P. S. (1976) *Struct. Bonding (Berlin)* **26,** 1–42.
25. Satterlee, J. D., Teintze, M. & Richards, J. H. (1978) *Biochemistry* **17,** 1456–1462.
26. Fuchsman, W. H. & Appleby, C. A. (1979) *Biochemistry* **18,** 1309–1321.
27. Findsen, E. W., Simons, P. & Ondrias, M. R. (1986) *Biochemistry* **25,** 7912–7917.
28. Chance, M. R., Campbell, B. F., Hoover, R. & Friedman, J. M. (1987) *J. Biol. Chem.* **262,** 6959–6961.
29. Campbell, B. F., Chance, M. R. & Friedman, J. M. (1987) *J. Biol. Chem.* **262,** 14885–14890.
30. Peng, S. M. & Ibers, J. A. (1976) *J. Am. Chem. Soc.* **98,** 8032–8036.
31. Scheidt, W. R., Haller, K. J., Fons, M., Mashiko, T. & Reed, C. A. (1981) *Biochemistry* **20,** 3653–3657.
32. Case, D. A. & Karplus, M. (1978) *J. Mol. Biol.* **123,** 697–701.
33. Herman, Z. S., Loew, G. H. & Rohmer, M.-M. (1980) *Int. J. Quantum Chem., Quantum Biol. Symp.* **7,** 137–153.
34. Eaton, W. A. & Hofrichter, J. (1981) *Methods Enzymol.* **76,** 175–261.
35. Makinen, M. W. & Eaton, W. A. (1973) *Ann. N.Y. Acad. Sci.* **206,** 210–222.
36. Churg, A. K. & Makinen, M. W. (1978) *J. Chem. Phys.* **68,** 1913–1925.
37. Richardson, H. H. & Ewing, G. E. (1987) *J. Phys. Chem.* **91,** 5833–5835.
38. Nuzzo, R. G., Fusco, F. A. & Allara, D. L. (1987) *J. Am. Chem. Soc.* **109,** 2358–2368.
39. Marden, M. C., Hazard, E. S. & Gibson, Q. H. (1986) *Biochemistry* **25,** 2786–2792.
40. Cornelius, P. A., Steele, A. W., Chernoff, D. A. & Hochstrasser, R. M. (1981) *Proc. Natl. Acad. Sci. USA* **78,** 7526–7529.
41. Martin, J. L., Migus, A., Poyart, C., LeCarpentier, Y., Astier, R. & Antonetti, A. (1983) *Proc. Natl. Acad. Sci. USA* **80,** 173–177.
42. Chernoff, D. A., Hochstrasser, R. M. & Steele, A. W. (1980) *Proc. Natl. Acad. Sci. USA* **77,** 5605–5610.
43. Martin, J. L., Migus, A., Poyart, C., LeCarpentier, Y., Antonetti, A. & Orzag, A. (1982) *Biochem. Biophys. Res. Commun.* **107,** 803–810.
44. Szabo, A. (1978) *Proc. Natl. Acad. Sci. USA* **75,** 2108–2111.
45. Collman, J. P., Gagne, R. R., Reed, C. A., Robinson, W. T. & Rodley, G. A. (1974) *Proc. Natl. Acad. Sci. USA* **71,** 1326–1329.
46. Jameson, G. B., Rodley, G. A., Robinson, W. T., Gagne, R. R., Reed, C. A. & Collman, J. P. (1978) *Inorg. Chem.* **17,** 850–857.
47. Hoard, J. L. (1975) in *Porphyrins and Metalloporphyrins*, ed. Smith, K. M. (Elsevier, New York), pp. 351–358.